Available online at www.sciencedirect.com
ScienceDirect
Ceramics International 37 (2011) 3677–3686
CERAMICS INTERNATIONAL
www.elsevier.com/locate/ceramint

Preparation of ultrafine CsCl crystallites by combined cryogenic and room temperature ball milling

C.S. Tiwary [a], Akash Verma [b], Krishanu Biswas [b,*], Amit K. Mondal [a], Kamanio Chattopadhyay [a]

[a] Department of Materials Engineering, Indian Institute of Science, Bangalore 560012, Karnataka, India
[b] Department of Materials Science and Engineering, Indian Institute of Technology, Kanpur 208016, UP, India

Received 16 January 2011; received in revised form 13 June 2011; accepted 16 June 2011
Available online 24 June 2011

Abstract

The present investigation reports the preparation and microstructural characterization of ultrafine CsCl crystallites using combined cryogenic and room temperature (RT) mechanical milling. The milling has been performed in evacuated WC vials under high purity argon atmosphere. The low temperature milling has been utilized as an effective means of rapid fracturing of the CsCl crystallites. This was followed by RT milling for different time durations. The final crystallite size obtained is 10 ± 6 nm for sample cryo-milled for 11 h and subsequently RT milled for 35 h. The experimental findings indicate the strong effect of duration of cryo-milling on the final size of the crystallites. The prolonged room temperature milling leads to increase of the crystallite size due to deformation-induced sintering. The results have been discussed in the light of currently available literature.
© 2011 Elsevier Ltd and Techna Group S.r.l. All rights reserved.

Keywords: A. Sintering; CsCl; Cryogenic temperature; Ball milling; Nanocrystallites

1. Introduction

Cesium chloride (CsCl), the family member of alkali halides (AH), is one of the most popular and important materials for mankind from ancient times. A great deal of research work on CsCl has been carried out in various fields of science and engineering due to its useful optical properties, i.e., the presence of colour centres [1,2]. The alkali halides with colour centres are considered to be promising systems for applications in new optical devices such as waveguides and nanolaser (nanometer-sized crystallites for lasing). The nanolasers are deemed to be a key element in realizing an optical computer on a single-semiconductor chip or any integrated optical fibre communication devices [3]. The fabrication of nanolasers requires preparation of nanocrystalline CsCl. The molecular beam epitaxy (MBE) techniques have made it possible to produce various types of nanostructures consisting of CsCl [4]. It has attracted lots of attention because of tremendous potentials for the purpose of miniaturizing electronic devices [5]. Thus, preparation and characterization of nanocrystalline CsCl is utmost important for application of such devices.

The ultrafine CsCl can be prepared by several experimental techniques. This includes both bottom-up and top-down approaches of nanomaterials production [4]. MBE, as mentioned earlier comes under the former category. Alkali halides are very reactive and therefore, chemical synthesis processes cannot be utilized for preparation of ultrafine CsCl. The most common technique utilizing the top-down approach is the mechanical milling. This process is carried out in a high-energy ball mill. It involves repeated deformation, cold-welding, fracturing and dynamic recrystallization to obtain ultrafine nanoparticles [6]. The impact force exerted by the balls on the powder causes plastic deformation leading to strain hardening and ultimately fracture. The main advantage of this process is the reduction of crystallite size to nanometric regime. A large volume of research work has been carried out on the preparation of metallic, oxide, nitride, boride nanocrystallites using ball milling. To the best of the authors' knowledge, a very few research work has been reported in the literature on preparation and characterization of halide nanocrystals [7]. The

* Corresponding author. Tel.: +91 512 2596184; fax: +91 512 2597505.
E-mail address: kbiswas@iitk.ac.in (K. Biswas).

0272-8842/$36.00 © 2011 Elsevier Ltd and Techna Group S.r.l. All rights reserved.
doi:10.1016/j.ceramint.2011.06.029

present work reports, for the first time, the preparation and detailed microstructural characterization of CsCl nanocrystallites by combined cryogenic and room temperature ball milling.

Cryo-milling is a kind of mechanical milling in which metallic or ceramic powders are ball milled in liquid-nitrogen (LN_2) slurry or at cryogenic temperatures. It is well known that the cooling of powders is an effective way to accelerate the fracturing process [9–11]. The extremely low temperature in cryo-milling suppresses recovery and recrystallization processes, causing rapid grain refinement [9]. It has been shown by Mohamed et al. [12] that the ultimate grain size obtained in the mechanical milling is determined by balance of following factors: (i) defect generation and (ii) recovery and recombination of defects during plastic deformation. The defect generation and the recovery kinetics are strong function of temperature [11]. It is well know that dynamic recovery can effectively be suppressed by low temperature milling for many materials [10]. On the other hand, at extremely low temperature, the plastic deformation is very limited and therefore, defect generation and recombination are not sufficient to obtain finer grain size. RT milling will lead to generation as well as annihilation of defects such as dislocations. Therefore, it is expected that combined cryo and RT milling will cause refinement of grain size. In the present investigation, such a study is carried out on CsCl, which is brittle at low temperature [2]. The idea of the using combined cryo and RT milling also originates from our previous study on preparation of nanocrystalline KCl crystallites using RT milling under Ar atmosphere [11]. The results of the investigations reveal that the crystallite size cannot be reduced below 90 nm even after 30 h of RT milling of KCl [11]. In fact, longer RT has been found to cause increase of crystallite size due to sintering.

2. Experimental details

Pure CsCl powder (Merck, Germany) was ball milled in a modified P0 (Pulverisette, Fritsch, Germany) mill using four 15-mm-diameter tungsten carbide (WC) balls in WC vial. The ball to powder weight ratio was kept as 20:1 at low temperature (77 K) as well as room temperature (RT). The low temperature in the vial was created by pouring a mixture of liquid nitrogen (LN_2) and methanol in an annular jacket around the vial. The powder in vial was not in contact with LN_2, thereby there was no contamination from coolant. The temperature of the sample was measured by resistance temperature detector (RTD) probe attached to the vial. The vials loaded with powder and ball, were evacuated using a vacuum pump to a pressure of 10^{-2} mbar before backfilling with argon gas. Milling was stopped intermittently to ensure the vacuum in the vial. Cryo-milling times ranged from a few hours to 11 h. The room temperature milling (RT milling) was carried out in the same mill with similar milling parameters. The milling time in RT milling was varied from few hours to 55 h. The samples taken out at different time durations were stored in the vacuum desiccators. Sufficient care had been taken to ensure that no contamination taking place during milling.

The milled powders were examined by X-ray diffraction technique using a Pan analytical Xpert Pro X-ray powder diffractometer with Cu Kα radiation (λ = 0.154056 nm). The peak shift was corrected using Si as an external standard. Before recording the XRD pattern of the milled CsCl powder, Si was sprinkled on the powder sample to precisely record the peak shift of the CsCl peaks due to mechanical milling. Microstructural analysis was performed using Scanning electron microscope, SEM (FEI SIRION XL 40 SFEG) operating at 5 kV and transmission electron microscope, TEM (Technai F30) operating at 100 kV. As radiation damage had been a problem for observation of CsCl in TEM, sufficient care had been taken to minimize radiation damage. The milled CsCl powders were mounted on Cu-grid of high mesh number (600 mesh size) so that charging could be avoided. Working quickly at low intensity (smaller condenser aperture) and at lower accelerating voltage had not been sufficient enough to obtain good quality images with minimum radiation damage. The samples were cooled to liquid nitrogen temperature using a cryo-holder (Gaton, PA, USA) to obtain good quality images.

3. Results

3.1. X-ray diffraction

Fig. 1 depicts the X-ray diffraction patterns of milled CsCl samples for different milling conditions. The positions of all the peaks are marked at the bottom of the figure. The Si peaks are marked by dashed lines. Si is used as an external standard to determine the peak shift due to size reduction and strain in the milled powder. All the other peaks in the diffraction patterns can be indexed using the reflections of CsCl. Therefore, the presence of any contaminants cannot be detected in the milled powder.

3.2. Scanning electron microscopy (SEM)

Now let us discuss the microstructural evolution of CsCl powder during ball milling. We have carried out cryo and RT milling of CsCl powder for different durations to study the effects of milling hours on final crystallite size. The process of mechanical milling of powders normally involves repeated welding, fracturing and rewelding of powder particles. This leads to reduction of crystallite size due to plastic deformation [6,8–10,12]. Fig. 2a is the SEM micrograph of the starting powder showing large particles (50–150 μm) with irregular morphology. As compared to the starting microstructure, several important characteristics can be observed in cryo-milled powders. Fig. 2b shows scanning electron micrograph (SEM) of powder cryo-milled for 7 h with insets showing magnified image. It is clearly observed that the particle size (1–2 μm) has extensively been reduced during cryo-milling as shown in the inset of Fig. 2b revealing small crystallites. One can also observe the presence of the fragmented finer crystallites as indicated by white arrows on the higher magnification micrograph. Fig. 2c is the representative

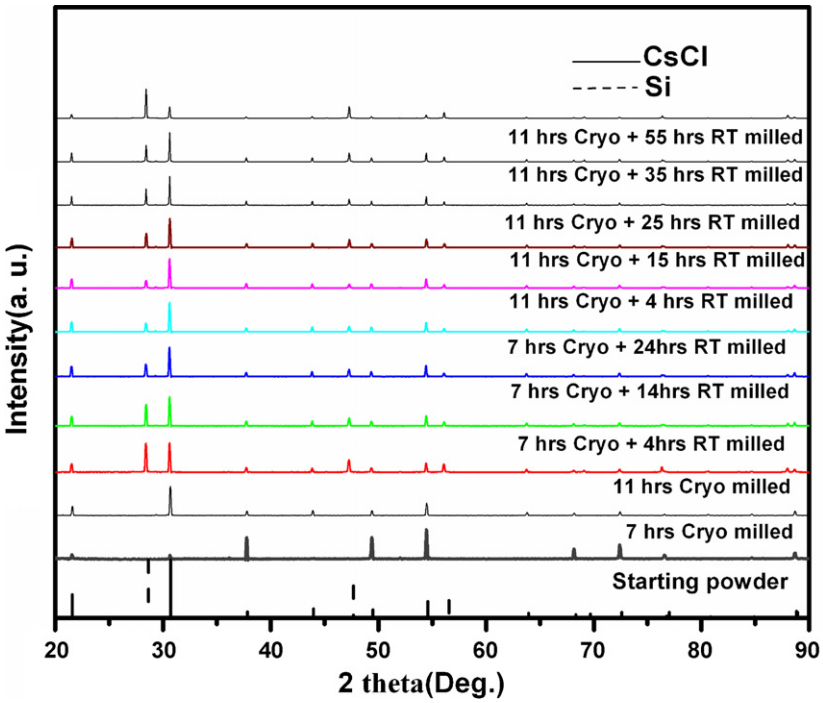

Fig. 1. XRD patterns of the NaCl milled at different times using cryo and RT milling. The peak positions for CsCl and Si are marked by solid and dashed lines respectively at the bottom.

micrograph of 11 h cryo-milled sample. The particle size has been found to be further reduced. The inset (white arrows on the magnified micrograph) reveals finer scale particles with larger particles. The particle size shows a bimodal distribution for both 7 h as well 11 h cryo- milled sample. Therefore, the micrographs suggest that bigger particles have been fractured and the fragmented pieces are formed during cryo-milling. The fragmented pieces are found to be fine scale.

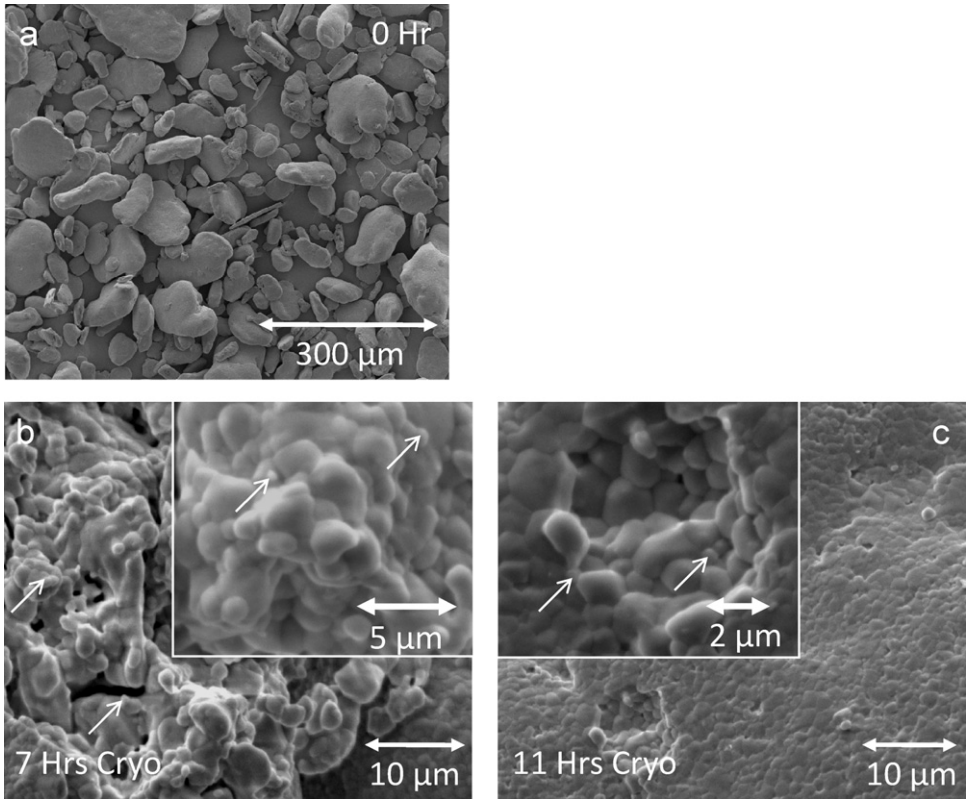

Fig. 2. SEM micrographs of CsCl powders cryo-milled for different time scales: (a) 0 h; (b) 7 h; (c) 11 h. The insets in (b) and (c) show higher magnification micrographs.

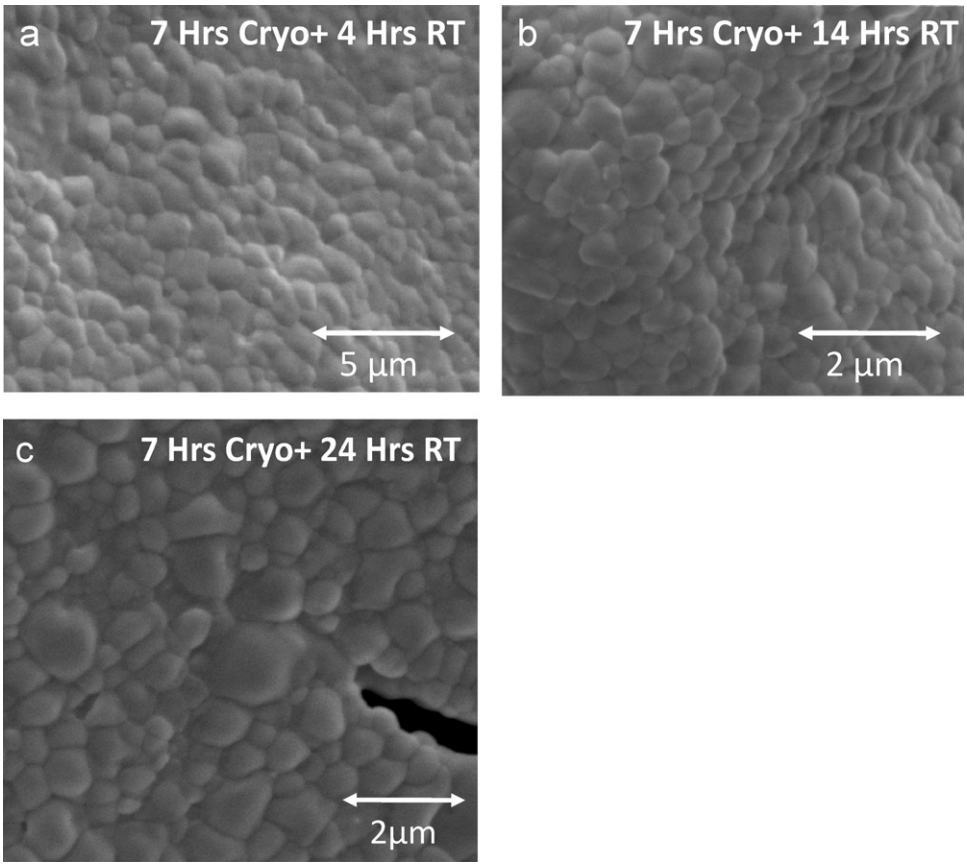

Fig. 3. SEM micrographs of the milled powders: (a) 7 h of cryo with 4 h of RT milling, (b) 7 h of cryo-milling and 14 h of RT milling and (c) 7 h cryo-milling and 24 h of RT milling.

The SEM observation of both the cryo-milled samples, which are subsequently room temperature (RT) milled for different time scale will be discussed now. We shall present here some representative micrographs. Fig. 3a shows the SEM micrograph of powder cryo-milled for 7 h followed by 4 h of RT milling. The micrograph illustrates the distribution of the particles in the size range of 0.5–3 μm with irregular shapes. Fig. 3b and c shows the SEM micrographs of samples cryo-milled for 7 h and subsequently RT milled for 14 and 24 h respectively. It is clear that longer room temperature milling causes further reduction of particle size. However, the micrograph in Fig. 3c illustrates the bimodal distribution of the particles with the smallest one of 0.2 μm and the biggest one being 5 μm. The shape of the crystallites remains irregular during RT milling.

Fig. 4 depicts SEM micrographs of the sample cryo-milled for 11 h and subsequently RT milled for different time duration. RT milling for 5 h leads to formation finer CsCl particles with bimodal distribution (Fig. 4a). Upon increasing the time of RT milling to 15 and 35 h, the microstructures (Fig. 4b and c) show concomitant decrease in particle size. The smallest particle size (0.2–0.3 μm) could be obtained by 35 h of RT milling. However, longer RT milling of 55 h leads to further increase of particle size (Fig. 4d). The shape of the particles remains irregular.

3.3. Transmission electron microscopic (TEM) observation

We have done detailed TEM characterization of all the samples. It has already been reported that the radiation-induced damage during TEM observations leads to charging problem [13]. The TEM was operated at lower accelerating voltage (100 kV) with minimum beam current. The smaller condenser aperture (2 μm) was used and the first condenser aperture was fully excited to obtain maximum beam diameter on the specimen to minimize beam-induced volatilization. All the TEM observations have been performed using liquid nitrogen cooled cryo-holder to obtain good quality images. Fig. 5a shows bright field image of sample cryo-milled for 7 h revealing different CsCl crystallites. One can observe that the most of crystallites reveals spherical or near spherical morphology. However, detailed TEM observations from different regions of the sample indicate the presence of some faceted crystallites. The inset shows a higher magnification bright field micrograph of one such crystallite oriented along [0 0 1] direction. The crystallite is found to be bounded by {1 0 0} facets. The crystallite size distribution has been calculated by generating histogram of crystallite size using the bright field micrographs. Measurements are carried out on at least 1 0 0 crystallites from TEM bright field micrographs to arrive at size distribution. The inset at bottom of Fig. 5a reveals

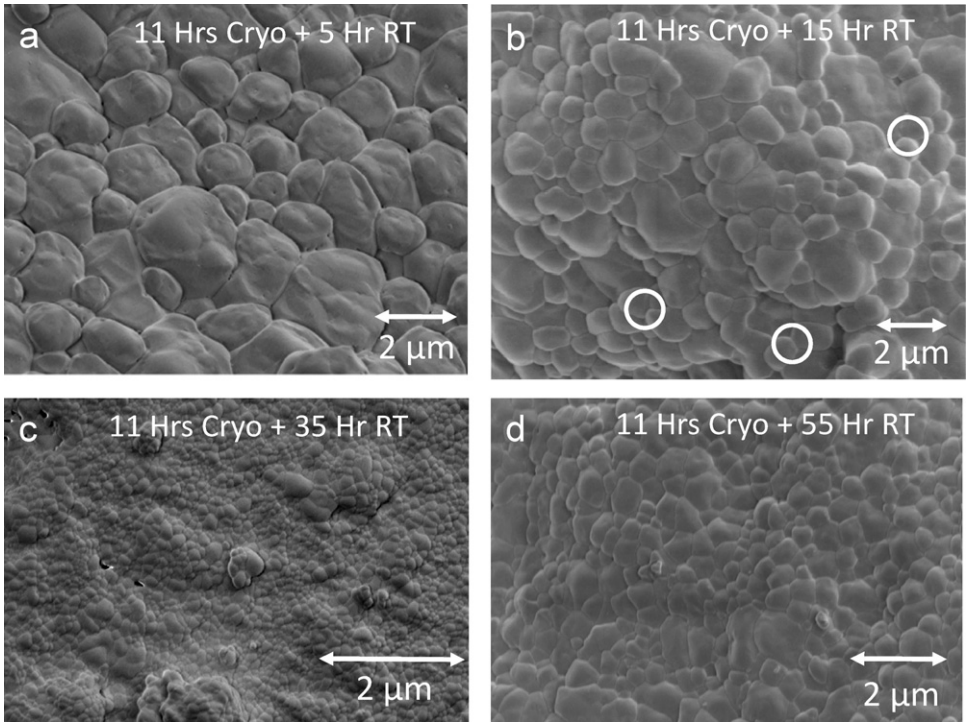

Fig. 4. SEM micrographs of the milled powders: (a) 11 h of cryo with 5 h of RT milling, (b) 7 h of cryo-milling and 15 h of RT milling (c) 7 h cryo-milling and 35 h of RT milling and (d) 11 h of cryo-milling and 55 h of RT milling.

the detailed crystallite size distribution. The average crystallite size is found to be 227 ± 36 nm. There are few crystallites in the size range of 100–150 nm. Fig. 5b shows bright field micrograph of powder cryo-milled for 11 h. The top inset shows higher magnification bright field micrograph of one such crystallite (size ∼80 nm). The micrograph has been obtained by orienting the particle along [0 0 1] zone axis. It shows near spherical shape of the crystallite. The crystallite size has indeed been reduced during milling that can be observed in the histogram (the bottom inset of Fig. 5b). The average crystallite size is 107 ± 23 nm. The large fraction of crystallites are having size <100 nm.

TEM observation of cryo-milled and subsequently room temperature milled samples are shown in Fig. 6. Fig. 6a is bright field micrographs of powder cryo-milled for 7 h and subsequently RT milled for 14 h. The average crystallite size of sample cryo milled for 7 h and RT milled for 14 h is 60 ± 18 nm. The crystallites retain near cuboidal shape (some of them are marked by white arrows in the figure). The low magnification bright field micrograph of the sample cryo-milled for 7 h and subsequently RT milled for 24 h is also shown in Fig. 6b with bottom inset showing the size distribution of the crystallite. The histogram reveals the mean crystallite size to be 36 ± 11 nm. There are a large number of crystallites having size more than 30 nm. The upper inset shows a higher magnification bright field micrograph of one of the crystallites (∼40 nm). The micrograph has been obtained with the particle oriented along [0 0 1] direction. It can be clearly observed that some of {1 0 0} facets of CsCl have been replaced by rough surfaces with pronounced roughening of the corners (marked by broken white arrows). Fig. 6c reveals the bright field micrograph of the sample cryo-milled for 11 h and subsequently RT milled for 15 h. The crystallite size has been further reduced (average crystallite size = 25 ± 10). The inset is a higher magnification micrograph of 22 nm sized CsCl crystallite when the crystallite has been oriented along [0 0 1] direction. One can clearly see that roughening of {1 0 0} facets with steps (marked by white arrows) generated along the facets. Fig. 6d shows the bright field micrograph of the sample cryo-milled for 11 h followed by RT milling of 25 h. The crystallites are found to be very fine with average crystallite size being 20 ± 7 nm. The inset shows higher magnification bright field micrograph of a 25 nm size crystallites oriented along [0 0 1] direction. The crystallite appears to be near spherical with large number of surface steps. The bright field micrograph obtained from the sample cryo-milled for 11 h and subsequently RT milled for 35 h is shown in Fig. 6e. One can observe the presence of ultrafine crystallite with inset showing one such crystallite oriented along [0 0 1] direction. The crystallites have irregular morphology. The histogram generated from large number of crystallites is shown as bottom inset. The average crystallite size is found to be 10 ± 6 nm. Longer room temperature milling leads to increase of the crystallite size. Fig. 6f reveals bright field micrograph of the sample cryo-milled for 11 h and subsequently RT milled for 55 h. The average crystallite size is found to be 21 ± 8 nm. It can be clearly observed that the crystallite size has been increased. Table 1 shows the average crystallite size obtained from TEM bright field TEM micrographs of CsCl samples under different milling conditions.

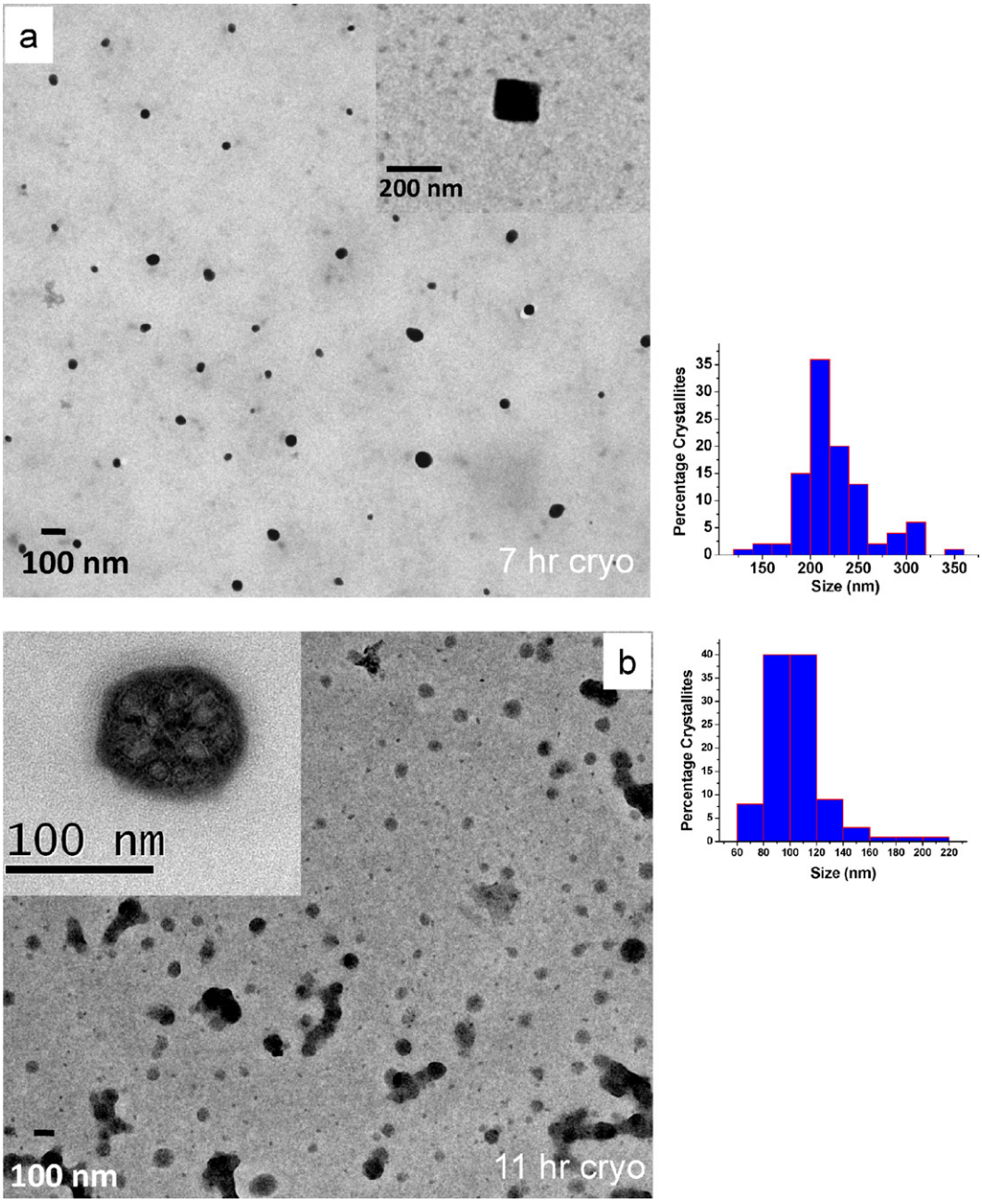

Fig. 5. Bright field TEM micrographs of the milled powders: (a) 7 h of cryo-milling and (b) 11 h of cryo-milling.

Table 1
Average crystallite size of CsCl mechanical milled under different milling conditions.

Mechanical milling conditions	Average crystallite size (nm)
7 h cryo	227 ± 36
11 h cryo	107 ± 23
7 h cryo + 4 h RT	90 ± 12
7 h cryo + 14 h RT	60 ± 18
7 h cryo + 24 h RT	36 ± 11
11 h cryo + 5 h RT	60 ± 12
11 h cryo + 15 h RT	25 ± 10
11 h cryo + 25 h RT	20 ± 7
11 h cryo + 35 h RT	10 ± 6
11 h cryo + 55 h RT	21 ± 8

4. Discussion

The present investigation has conclusively shown that the ultrafine CsCl crystallite can be prepared by using combined cryo and room temperature (RT) mechanical milling. The duration of cryo-milling, prior to RT milling, plays a crucial role in deciding final crystallite size in the nano-regime. In the following, we shall discuss the efficacy of combined milling in the light of available literature.

During mechanical milling, the powder experiences severe plastic deformation due to the action of balls, which basically causes the grain refinement. This process leads to transformation of a plastic-deformation induced dislocation structure to

high-angle grain boundaries [6,8–10,12]. Microscopically, the formation of nanocrystalline grains by mechanical milling involves three stages [14]. At the beginning, severe plastic deformation is applied to the powder. The deformation thus induced, is localized into shear bands containing a high density of dislocation network, which therefore causes the increase of the plastic strain. In the subsequent stage, the larger grains are disintegrated into sub-grains separated by low-angle grain boundaries due to successive accumulation of dislocations in the microstructure. The formation of sub-grains is mainly due to the process of annihilation and recombination of dislocations by polygonization [10]. In the final stage, the continued deformation leads to formation of additional shear bands with associated reduction of sub-grain size and reorientation of final grains with high-angle orientation. Therefore, the dislocation generation, accumulation and annihilation are bare necessity

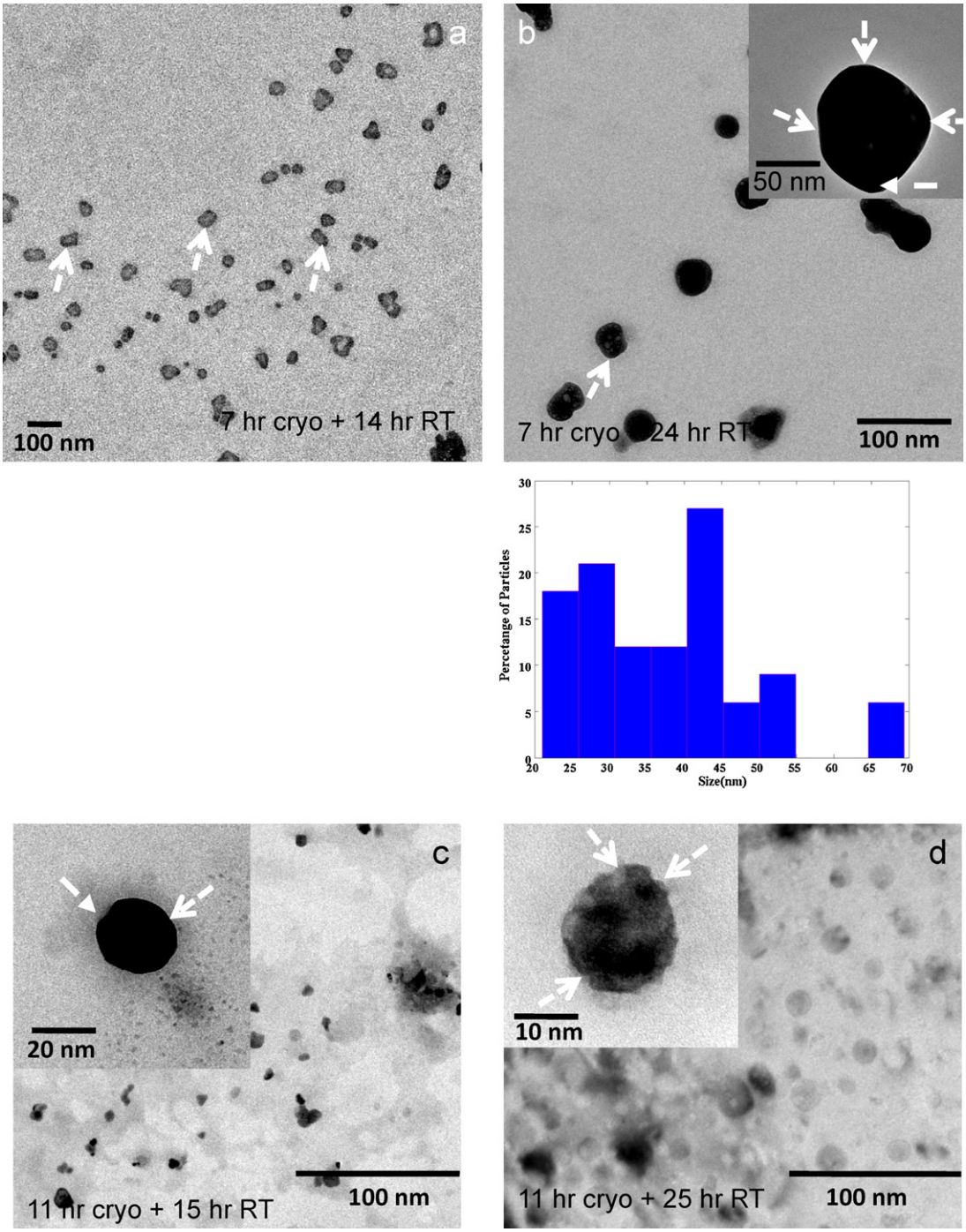

Fig. 6. Bright field TEM micrographs of the milled powders: (a) 7 h of cryo-milling and 14 h of RT milling; (b) 7 h of cryo-milling and 24 h of RT milling; (c) 11 h of cryo-milling and 15 h of RT milling; (d) 11 h of cryo-milling and 25 h of RT milling; (e) 11 h of cryo-milling and 35 h of RT milling and (e) 11 h of cryo-milling and 55 h of RT milling. The top inset in (b)–(e) reveals higher magnification micrograph of one crystallite whereas bottom inset of (b) and (e) shows crystallite size distribution.

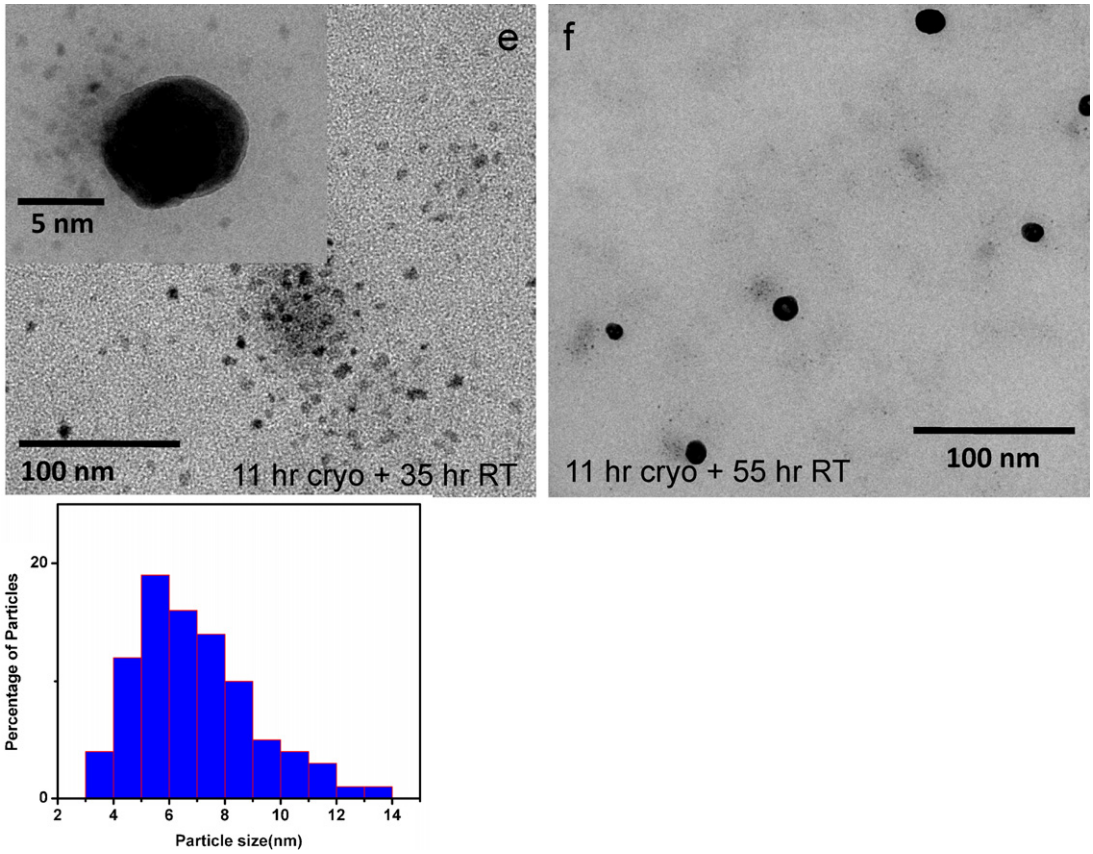

Fig. 6. (*Continued*).

for grain refinement during mechanical milling [9,10,12]. It has already been shown [12] that the ultimate crystallite size depends on hardening rate which is induced by dislocation generation and recovery rate due to dislocation annihilation and recombination. These two factors depend upon the ability of a material to be plastically deformed at cryogenic and room temperature during mechanical milling. For a brittle material like CsCl, the factors governing grain refinement during mechanical milling is the temperature-dependent mechanical properties. To the best of the authors' knowledge, the mechanical properties of CsCl at low (cryogenic) temperatures are not available in the literature. However, it is well known that CsCl is a brittle polycrystalline material at RT [2]. It has been discussed earlier that the fine-scale nanostructured CsCl crystallites cannot be prepared without build up of a plastic-deformation-induced dislocation structure [8]. For CsCl, it is easier to initiate plastic deformation by mechanical milling at RT than at cryogenic temperatures. Therefore, it is clearly understood that a combined cryo and RT milling will be effective for the preparation of nanocrystalline CsCl. At cryogenic temperatures, little plastic deformation occurs in the CsCl crystallites and failure mostly occurs by defects such as microcracks. Therefore, cooling the powder to cryogenic or close to cryogenic temperatures is an effective means to accelerate the fracturing process. Fig. 7a is a high resolution micrograph of the CsCl crystallite cryomilled for 11 h showing evidence no visible defect in the sample. The low magnification TEM micrographs of same sample (not shown here) do not reveal presence of dislocations, signifying no visible plastic deformation in the sample during cryo-milling.

RT milling of CsCl will likely to increase of temperature beyond which plastic deformation activity is possible. Therefore, it is important to know the temperature of powder during ball milling. The temperature of WC vial was monitored using a RTD sensor attached to the vial. The peak temperature recorded was 65 °C. It has been reported in the literature that the local temperature increase during the collisions of the balls with powder will be much higher than the vial temperature. Schwarz and Koch [15] have analyzed the temperature increase resulting from the local shear of the powder entrapped between the balls during mechanical milling as

$$\Delta T = \frac{F}{2}\left(\frac{\Delta t}{\pi k \rho c_P}\right)^{1/2}, \tag{1}$$

where ΔT = temperature increase, F = dissipated energy flux = σV_r, σ = normal stress caused by a head-on collision, V_r = relative velocity of the balls before the impact, Δt = stress state life time, ρ = density of powder, k = thermal conductivity and C_P = heat capacity of powder. We can assume that the normal stress generated by a head-on collision of two balls of diameter d, which is given by [16]

$$\sigma = \sigma_C = 0.616\left\{PE^2\left(\frac{2}{d}\right)^2\right\}^{1/3}, \tag{2}$$

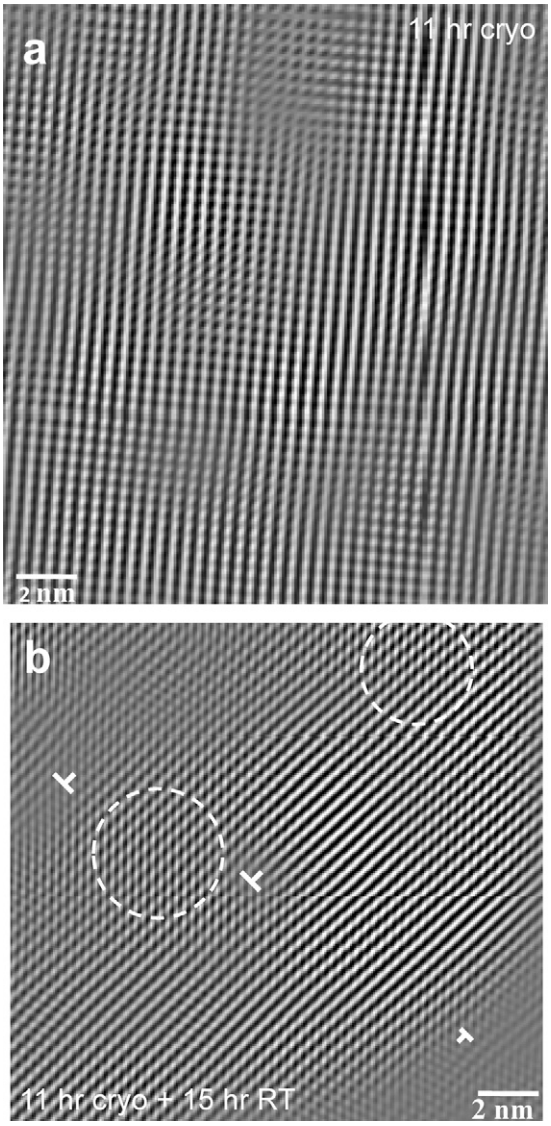

Fig. 7. HRTEM micrographs of the milled CsCl powder: (a) 7 h of cryo-milling and (b)7 h of cryo-milling and subsequently RT milled for 25 h.

where E = the elastic modulus of the balls, P = load. Using the values given in Table 2 for CsCl and V_r = 20 m/s, Δt = 1 ms, the calculated value of ΔT = 705 K (430 °C). Therefore, it is likely that the temperature of CsCl crystallites will be much higher than the temperature required for plastic deformation. Thus, this temperature rise would cause plastic deformation of CsCl during RT milling. Fig. 6b shows a high-resolution micrograph of a CsCl crystallite prepared by 7 h of cryo-milling followed by RT milling of 24 h. The micrograph reveals the presence of dislocations (marked in Fig. 7b). The calculation using a large number of high resolution micrographs indicate the dislocation density of $1.6 \times 10^{16}/cm^2$ in the sample. Therefore, the mechanisms responsible for mechanical milling of a ductile material can be applied to RT milling of CsCl after cryo-milling [8]. The mechanical milling will cause the localized deformation with shear bands containing high density of dislocations as seen in Fig. 7b. For reduction of crystallite size, the accumulation of dislocation within the existing deformed grains is necessary.

Table 2
Physical and mechanical properties of CsCl.

Properties	Values	Ref.
Density, ρ (kg/m^3)	3990	[20]
Melting temperature, T_m (K)	918	[20]
Elastic modulus, E (GPa)	23.8	[21]
Heat capacity, C_P (J/mol K)	3877.3	[22]
Thermal conductivity, k (W/mK)	0.6	[23]
Diameter of WC ball, d (m)	0.015	
Density of WC, ρ_{WC} (kg/m^3)	15,600	[24]

These dislocations then annihilate and recombine to form subgrains, leading to decrease in strain induced by ball milling. Normally, the plastic strain of the accumulated dislocations is reduced by a process called polygonization – a low energy configuration of dislocation of similar signs. Several investigators [17] have studied the process of polygonization in the alkaline halides and have concluded that the first stage of polygonization required the temperature to be increased to 27 °C. Therefore, the preceding discussion clearly tells us that the preparation of ultrafine nanocrystalline CsCl crystallites requires combined cryo and RT milling.

An important observation of the present investigation is the bimodal size distribution of the crystallite size for longer duration of RT milling (Figs. 4d and 6f). It has been observed that the microstructure consists of few larger size particles with large number of smaller ones. This can be attributed to sintering of CsCl crystallites during ball milling with temperature rise and plastic deformation aiding the sintering. The sintering of CsCl crystallites can occur due to temperature-enhanced plastic deformation as well as microdiffusion during RT mechanical milling. It has been reported in the literature [18] that surface and volume diffusion, plastic deformation and evaporation condensation are three basic mechanisms for sintering of halide crystallites. Detailed microstructural characterization using SEM indicate the formation of numerous inter-particle necking (Fig. 4b). The presence of few necks is marked on the figure. Such observations have also been reported by Davis et al. [8] for milling of brittle couples Si–Ge. The densification of halides in the early stage is due to plastic deformation, which is followed by diffusion aided sintering [19]. We have already discussed about the local temperature rise of 430 °C (~0.77 T_m) for the CsCl particles during RT milling. This temperature increase will cause enhanced plastic deformation as well as diffusion by defect generation. The decrease of crystallite size during milling can cause a substantial increase in the grain-boundary area, making the grain boundary-diffusion at elevated temperature the dominant sintering mechanism.

5. Conclusion

In summary, the combined cryo and room temperature mechanical milling is found to be very effective in formation of ultrafine CsCl crystallites. The low temperature milling has been utilized as an effective means for rapid fracturing of CsCl particles. On the other hand, RT milling leads to temperature

rise of 430 °C, which is sufficient for dislocation activity in the crystallite. The detailed microstructural study using SEM and TEM show several features. The formation of bigger crystallites can be explained due to sintering of smaller CsCl crystallites aided by plastic deformation as well as grain boundary diffusion.

Acknowledgement

The authors would like to acknowledge Nanoscience and Technology Initiatives (NSTI) of Department of Science and Technology (DST), Govt. of India for funding.

Appendix A. Supplementary data

Supplementary data associated with this article can be found, in the online version, at doi:10.1016/j.ceramint.2011.06.029.

References

[1] G. Yoshikawa, M. Kiguchi, K. Ueno, A. Koma, K. Saiki, Visible light photoemission and negative electron affinity of single crystalline CsCl thin films, Surf. Sci. 544 (2003) 220–226.
[2] W.P. Davey, Precision measurements of crystals of the alkali halides, Phys. Rev. 21 (1923) 143–161.
[3] M. Cameron, J.A.M. Pereira, S. Pelli, G.C. Righini, Optical waveguides produced in LiF by MeV ion beam bombardment, Appl. Phys. Lett. 81 (2002) 4103–4105.
[4] S. Asaka, M. Itoh, M. Kamada, Ultraviolet light amplification within a nanometer-sized layer, Phys. Rev. B 63 (2001) 081104–81111.
[5] S. Fölsch, A. Helms, S. Zophel, J. Repp, G. Meyer, K.H. Rieder, Self-organized patterning of an insulator-on-metal system by surface faceting and selective growth: NaCl/Cu(2 1 1), Phys. Rev. Lett. 84 (2000) 123–126.
[6] B.S. Murty, S. Ranganathan, Novel materials synthesis by mechanical alloying/milling, Int. Mater. Rev. 43 (1998) 103–141.
[7] A. Verma, K. Biswas, C.S. Tiwary, A.K. Mondal, K. Chattopadhyay, Combined cryo and room temperature ball milling to produce ultrafine halide crystallites, Metall. Trans. A 42A (2011) 1127–1137.
[8] R.M. Davis, B. McDermott, C.C. Koch, Mechanical alloying of brittle materials, Metall. Trans. A 19 (1988) 2873–2874.
[9] K.H. Chung, J. Lee, R. Rodriguez, E.J. Lavernia, Grain growth behaviour of cryo-milled INCONEL 625 powder during isothermal heat-treatment, Mater. Met. Trans. A 33 (2002) 125–134.
[10] B. Han, J. Ye, F. Tang, J. Shoenung, E.J. Lavernia, Processing and bahaviour of nanostructured metallic alloys and composites by cryo-milling, J. Mater. Sci. 42 (2007) 1660–1672.
[11] P. Sharma, K. Biswas, K. Chattopadhyay, Size effect on the lattice parameter of nanosized KCl crystallites, Scripta Mater. 61 (2009) 600–603.
[12] E.J. Lavernia, B.Q. Han, J.M. Schoenung, Cryomilled nanostructured materials: processing and properties, Mater. Sci. Eng. A 493 (2008) 207–214; F.A. Mohamed, A dislocation model for the minimum grain size obtainable by milling, Acta Mater. 51 (2003) 4107–4119.
[13] L.W. Smiser, T.D. McGee, Transmission electron microscopy of sodium chloride, J. Am. Soc. – Discuss. Notes 52 (12) (1969) 681–682.
[14] H.J. Fecht, Nanostructure formation by mechanical attrition, Nanostruct. Mater. 6 (1995) 33–42.
[15] R.B. Schwarz, C.C. Koch, Formation of amorphous alloys by the mechanical alloying of crystalline powders of pure metals and powders of intermetallics, Appl. Phys. Lett. 49 (1986) 146–148.
[16] R.J. Roark, Formulas for Stress and Strain, McGraw-Hill Book Co., Inc., New York, 1954, p. 275.
[17] S. Amelinckx, R. Strumane, Geometry and kinetics of the polygonization of sodium chloride, Acta Metall. 8 (1960) 312–320.
[18] W.D. Kingery, M. Berg, Study of the initial stages of sintering solids by viscous flow, evaporation–condensation, and self-diffusion, J. Appl. Phys. 26 (10) (1955) 1205–1212.
[19] R. Goodall, J.-F. Despois, A. Mortensen, Sintering of NaCl powder: mechanisms and first stage kinetics, J. Appl. Phys. 31 (3) (1960) 488–493.
[20] L.R. David (Ed.), Handbook of Chemistry and Physics, 91st ed., CRC Press, Boca Raton, FL, 2011, pp. 4–67.
[21] D.B. Sirdeshmukh, L. Sirdeshmikh, K.G. Subhadra (Eds.), Alkali Halides – A Handbook of Physical Properties, Springer Series in Materials Science, Berlin, 2001.
[22] M.J.V. Lourenco, F.J.V. Santos, M.L.V. Ramires, C.A. Nieto de Castro, Isobaric specific heat capacity of water and aq.CsCl solutions for temperature between 298 K and 370 K at $p = 0.1$ MPa, J. Chem. Thermodyn. 38 (8) (2006) 970–974.
[23] D. Gerlich, P. Anderson, Temperature and pressure effect on the thermal conductivity and heat capacity of CsCl, CsBr and CsI, J. Phys. C: Solid State Phys. 15 (1982) 5211–5222.
[24] K. Biswas, A. Muphopadhyay, B. Basu, K. Chattopadhyay, Processing and microstructure of WC–ZrO_2 nanocomposites, J. Mater. Res. 22 (6) (2007) 1491–1501.